AL/EQ-TR-1997-3104

COMPUTATIONAL FLUID DYNAMICS (CFD) ANALYSIS AND DEVELOPMENT OF HALON-REPLACEMENT FIRE EXTINGUISHING SYSTEMS (PHASE II)

D. Nickolaus

CFD Research Corporation
215 Wynn Drive
Huntsville, AL 35805

December 1997

ENVIRONICS DIRECTORATE
ARMSTRONG LABORATORY

■ **Air Force Materiel Command** ■ **United States Air Force** ■ **Tyndall Air Force Base, FL 32403-5323**

DISCLAIMER

Reference herein to any specific commercial product, process, or service by trade name, trademark, manufacturer, or otherwise does not constitute or imply its endorsement, recommendation, or approval by the United States Air Force. The views and opinions of authors expressed herein do not necessarily state or reflect those of the United States Air Force.

This report was prepared as an account of work sponsored by the United States Air Force. Neither the United States Air Force, nor any of its employees, makes any warranty, expressed or implied, or assumes any legal liability or responsibility for the accuracy, completeness, or usefulness of any information, apparatus, product, or usefulness of any information, apparatus, product, or process disclosed, or represents that its use would not infringe privately owned rights

This document is submitted as an historical record of work performed. Limitations of the available media rendered editing impractical; therefore it is retained “as is.”

REPORT DOCUMENTATION PAGE

Form Approved
OMB No. 0704-0188

PLEASE DO NOT RETURN YOUR FORM TO THE ABOVE ADDRESS.

1. REPORT DATE *(DD-MM-YYYY)*	2. REPORT TYPE	3. DATES COVERED *(From - To)*
01-DEC-1997	Final Technical Report	01-DEC-1996 -- 30-NOV-1997

4. TITLE AND SUBTITLE

Computational Fluid Dynamics (CFD) Analysis and Development of Halon-Replacement Fire Extinguishing Systems (Phase II)

5a. CONTRACT NUMBER

5b. GRANT NUMBER

5c. PROGRAM ELEMENT NUMBER

6. AUTHOR(S)

Nickolaus, D.

5d. PROJECT NUMBER

5e. TASK NUMBER

5f. WORK UNIT NUMBER

4398C28B

7. PERFORMING ORGANIZATION NAME(S) AND ADDRESS(ES)

CFD Research Corporation
215 Wynn Drive
Huntsville, AL 35805

8. PERFORMING ORGANIZATION REPORT NUMBER

CFDRC 4862B/2

9. SPONSORING/MONITORING AGENCY NAME(S) AND ADDRESS(ES)

Air Force Research Laboratory
Materials and Manufacturing Directorate
Airbase Technologies Division
139 Barnes Drive, Suite 2
Tyndall Air Force Base, FL 32403-5323

10. SPONSOR/MONITOR'S ACRONYM(S)

AL/EQ

11. SPONSOR/MONITOR'S REPORT NUMBER(S)

AL/EQ-TR-1997-3104

12. DISTRIBUTION/AVAILABILITY STATEMENT

Distribution A: Approved for public release; distribution unlimited.

13. SUPPLEMENTARY NOTES

Document contains color images.

14. ABSTRACT

Many Halon replacement fire extinguishing agents have been proposed and are being tested. Replacement agents have different properties than Halon, and thus perform differently in existing application hardware. Computational Fluid Dynamics (CFD) is ideally suited to analyze agent flow through application hardware and also agent flow after discharge from the hardware. In previous (Phase I) work, CFD Research Corporation developed a computational model for a 20 lb handheld fire extinguisher with Halon 1211. The model was improved in this Phase II work to more accurately reflect the pressure-density relationship of Halon 1211 in an expansion driven phase change. The model was used to investigate the velocity, pressure and gas/liquid mixture throughout the assembly. Benchmark data were also taken to calibrate the assembly, and velocities were measured at six location outside the nozzle. CFD analysis agrees with measurements fairly well. Pressure and velocity at the nozzle exit are in good agreement. However, the velocity decay 50 and 75 mm downstream of the nozzle exit are underpredicted. Causes of the underprediction are explained, and ways to improve th4e model in Phase III are discussed.

15. SUBJECT TERMS

Halon, fire extinguishing agents, computational model, handheld fire extinguisher

16. SECURITY CLASSIFICATION OF:			17. LIMITATION OF ABSTRACT	18. NUMBER OF PAGES	19a. NAME OF RESPONSIBLE PERSON
a. REPORT	b. ABSTRACT	c. THIS PAGE			Richard Brown
U	U	U	SAR	27	19b. TELEPHONE NUMBER *(Include area code)*

Reset

Standard Form 298 (Rev. 8/98)
Prescribed by ANSI Std. Z39.18

BACKGROUND

Halons have been the fire extinguishing agent of choice on military flight lines for many years. Halons have been shown to destroy the Earth's ozone and as a consequence, the Montreal Protocol and US EPA actions have mandated the phase-out of halon production and consumption. Several replacement agents have been proposed, such as hydrochlorofluorocarbons (HCFCs), perfluorocarbons (PFCs), and fluoroiodocarbons (FICs). In the case of many replacement agents, the fluid properties (density, boiling point, saturation pressure curve, heat of vaporization, etc.) of the replacements are quite different than the halon properties. These differing properties will have an impact on the transport characteristics of the agent; from the agent cylinder, through the distribution conduit and nozzle, and out to the fire.

The application performance of these new agents must be determined, but testing is very expensive. As a cost-effective alternative, CFD Research Corporation (CFDRC) is developing a CFD model to analyze and optimize application performance for a wide range of fluid properties and hardware geometries. By using CFD analysis as a supplement to experimental testing, the number of experimental tests can be dramatically reduced.

This report describes the work performed in Phase II activities. In Phase I, a preliminary CFD model of a 20 lb handheld fire extinguisher with Halon 1211 was developed and CFD software/hardware was delivered to the Air Force. In Phase II, work continued in the retirement of the CFD model along with the collection and analysis of benchmark experimental data.

BENCHMARK DATA

Six 20 lb fire extinguishers were borrowed from Amerex for benchmark testing. They were loaded with 20 lb Halon 1211 and charged to 190 psi by Tyndall AFB. One hose and nozzle assembly was instrumented and used with all six tanks. Wall static pressures were recorded at the hose inlet fitting (just downstream of the valve), at the mid-point of the nozzle orifice, and at the mid-point of the nozzle diverging section. Temperature was also measured at the latter location. Mass of halon in the tank was measured as well as halon droplet velocity at six locations downstream of the nozzle discharge. Testing occurred at Energy Research Consultants in Laguna Hills, CA. Figure 1 shows the test installation. Instrumentation at the three measuring planes listed above can be seen.

Halon mass decay for the tanks is shown in Figure 2. Mass shown is the difference between the instantaneous mass of the complete tank assembly and the mass when fully discharged. Liquid runout occurred between t=26 and 30 seconds. The mass decay slows down as halon mass nears zero. Each tank discharged in a slightly different manner. For example, tank 4 began with more mass and discharged at a higher rate than other tanks, while tank 6 discharged more slowly. For further analysis, all were averaged. The first 25 seconds were expressed with various curve fits. An exponential decay (often assumed for tank discharge) did not match data well. It had a correlation

coefficient of 0.971. A second order polynomial was much better at 0.999.

$m\ (lb) = 7.923e\text{-}3\ t^2 - 0.887\ t + 20.283$
so, $\partial m/\partial t = 0.887 - 0.01585\ t$

Pressure downstream of the valve (in hose inlet fitting) is shown in Figure 3. Again, differences between tanks can be noted. Tank 4 began at a higher pressure than others and discharged more rapidly. In all cases, the maximum pressure is quickly reached. A 50 psi drop from the tank charge pressure to the maximum hose inlet pressure is measured. A distinct knee in the pressure decay is indicative of liquid runout. This occurs at approximately 60 psig.

Pressure at the mid-point of the nozzle orifice (Figure 4) shows similar trends. Pressure rises very rapidly to a peak around 83 psig. Orifice pressure at liquid runout is 40-50 psig. Pressures at the nozzle mid-point (shown in Figure 5) never deviate much from atmospheric. Figure 5 shows a typical tank initially dropping to -0.6 psig, slowly rising to -0.2, and rapidly dropping to -1.4 at liquid runout. As pressure returns to atmospheric, pressure cycling is clear evidence of the "chuffing" observed during the tests. In the last half of the discharge, a fairly obvious cyclic surge was heard along with a small fluctuation in the included angle of the discharge spray.

Temperatures at the nozzle mid-point were measured with limited success. Most tank discharges ruined the thermocouple. A heavy duty but slow response TC was installed for the tank 4 discharge. Figure 6 shows that temperatures dropped to -8 °C and held constant until further dropping to a minimum of -30 °C at runout. This clearly indicates that the process is not iso-thermal. A small rim of frost developed on the outside of the nozzle end at the very end of each discharge.

Velocity measurements were taken during each tank discharge. A two-component phase Doppler interferometry (PDI) system was employed (Aerometrics Doppler Signal Analyzer). The sampling volume was aligned at a different location for each tank discharge, varying from 2.5 to 75 mm downstream of nozzle discharge and either on the centerline or slightly inside the outer border of the halon spray.

Table 1. Velocity Measurement Location

Tank	Axial Position (from nozzle exit) (mm)	Radial Position (from $\mathbb{C}_L$) (mm)
1	25	11
2	75	15.9
3	75	0
4	50	0
5	50	14
6	2.5	12.6

Serious difficulties were encountered with measuring the spray. The combination of very high droplet density and high velocity generated a droplet sampling frequency beyond anything Aerometrics factory personnel had ever encountered. As a result, most of the data from the first two tanks was lost.

All of the available data are plotted for each tank discharge. Figures 7 and 8 show the velocities available for tanks 1 and 2. Figures 9-12 show considerably more data for the remaining tanks. A common trend can be seen in each of them. Velocity begins high and tapers down by 40-70% within 8-10 seconds. It remains constant until liquid runout. At that point velocity surges and drops away. Up to 37,000 data points are plotted on one graph. The velocities on the centerline show some data scatter, but those near the outer edge of the spray show a tremendous range of velocity at each point in time.

This overwhelming amount of data was broken down for each tank. Relevant time periods were selected and velocity values were analyzed. Both arithmetic average and standard deviation were calculated for each time span. Results are shown in Table 2.

Table 2. Discharge Velocity Analysis

Time Span (sec)	Avg Velocity (m/s)	Std Deviation	# Data Points
Tank 1			
0-1	50.7	23.1	56
Tank 2			
0-2	23.1	8.6	8,000
Tank 3			
0-5	21.1	7.6	400
5-10	15.7	6.2	800
10-29	12.6	6.9	6,500
29-35	36.6	10.1	19,400
Tank 4			
0-1	36.7	11.7	100
1-5	27.8	9.2	300
5-10	17.8	9.1	700
10-25	11.1	8.9	2,300
25-31	37.8	11.4	17,500

Time Span (sec)	Avg Velocity (m/s)	Std Deviation	# Data Points
Tank 5			
0-1	28.2	5.6	7,500
1-5	25.5	6.6	12,900
5-8	19.4	8.9	3,100
8-26	18.5	10.9	8,400
26-30	31.4	11.6	4,900
Tank 6			
0-1	49.1	21.2	124
1-30	38.8	31.6	2,900
30-36	40.1	16.6	4,900

IMPROVEMENT OF CFD ANALYSIS CODE

The primary challenge for the CFD portion of this project was achieving a good representation of the pressure-density relation for Halon 1211. Figure 13 shows the sudden change and severe slope for the pressure-density relation, which was determined from enthalpy-pressure data. The approximation of linear relations used in Phase I are shown in color. None of the linear relations yield an exact fit to the actual curve. Improvement was needed in the cavitating liquid approach.

An new approach was formulated which allowed for a more exact fit to the pressure-density relation. A customized version of the analysis source code was written which calculated density of the halon/nitrogen mixture based on their concentrations, temperature and pressure. It broke the fluid's pressure-density curve into pieces. Both halon and nitrogen are treated as customized gases. At pressures above 3.1E5 the fluid is fixed at the liquid density of 1826.6 kg/m^3. Two fourth order polynomials were used to create the pressure-density relation between 1 and 3 atmospheres. This allowed a rounded corner at 2.8E5 (where phase begins to change rapidly) to be created. This greatly eased problems with sudden changes in the $\partial\rho/\partial P$ term. At pressures below 0.945 atmosphere, the fluid was coded to behave as an ideal gas. The four-part relation is shown in Figure 14 along with the desired density points from Figure 13. Since an ideal gas' density is inversely proportional to temperature, a temperature term was added to the polynomials such that for rho = $f(T)^n$, n=0 at 3 atm and n=1 at 1 atm.

This approach has the advantage of allowing both nitrogen and halon to be freely introduced in whatever proportions appropriate. The previous cavitating liquid approach treats all the halon as a liquid with a varying density and air as a standard ideal gas. This new gas-gas approach treats both halon and nitrogen as gases. A nearly

exact conformance to the desired pressure-density relation is achieved. The cavitation approach fixes all the halon at a constant enthalpy, whereas the gas-gas approach allows Cp to vary with temperature.

An attempt to simply add the extra code to account for the change in Cp from liquid to gas state was unsuccessful. This would likely have resulted in reduced temperatures in the nozzle where the phase change occurs. It is recommended that this code modification be performed in Phase III.

CFD RESULTS FOR FULL TANK PRESSURE

CFDRC set up an internal flow model for an Amerex 20 pound handheld extinguisher with Halon 1211. The computational geometry exactly reproduces the tank, diptube, valve, hose, and nozzle. The only variation from physical reality is the absence of the turn between the valve and hose. The geometry and boundary conditions for the model are essentially the same as were used in Phase I (see CFDRC Report 4862/1, March 1997). The overall grid is shown in Figure 15. The extended region downstream of the nozzle discharge, found to be of benefit in Phase I, was retained throughout this effort. The details of the orifice and nozzle are shown in Figure 16. All analysis assumed an ambient temperature of 300K.

One significant modification to the inlet boundary condition from Phase I was dropping the pressure from 1.9E6 Pa to 1.31E6 Pa. This change reflects the fact that a normal Halon 1211 tank is pressurized to 190 psi. Results of the quasi-steady analysis at 1.3E6 Pa nearly reproduce the conditions 0.3 seconds into a discharge where the hose is full and pressure in the hose is at a maximum.

Many of the observed results remain similar to those seen in Phase I. Pressure drops slowly through most of the assembly until the orifice. The orifice section takes most of the pressure drop in the system. Figures 17 and 18 show the pressure field for the complete assembly and an enlargement of the orifice/nozzle section. As a result of such a pressure field, velocities remain low upstream of the orifice (Figure 19). Flow accelerates into the reduced area of the orifice, and further accelerates in the nozzle because of the density reduction from the phase change. The expansion and phase change create a small recirculation behind what appears to be a normal shock 0.75" downstream of the orifice. The density changes (Figure 20) inside the nozzle conform to the shock structure and further decay of pressure toward ambient.

COMPARISON OF BENCHMARK DATA TO CFD RESULTS

The purpose for the benchmark data was to determine the accuracy of the CFD model. Based on the derivative of the halon mass equation, the maximum mass flow is 0.887 lb/s (at t=0). The CFD calculation yields a mass flow of 1.33 lb/s. The calculated mass flow could be high because the tank pressure is held at 190 psi, for the quasi-steady solution, while actual tank pressure will be reduced. Other factors could include effects of dissolved nitrogen in reducing density or other model refinements discussed below.

Pressure and temperature in the hose, orifice and nozzle were compared to CFD calculations at the corresponding locations. Measured velocities were also compared to calculated velocities in the extended region downstream of the nozzle. Comparisons were made with the measurements taken near 0.3 seconds. Pressure values are taken from six tank averages.

Table 3. Pressure Comparison

Location	Measured Pressure (psig)	Calculated Pressure (psig)
Hose inlet	140	165
Mid orifice	83	27
Mid nozzle	0	2

The difference at the hose inlet could be due to the calculations not reflecting the reduced tank pressure from filling the system. The orifice pressure however, is significantly underpredicted. This discrepancy is entirely contained within the converging section leading to the orifice. At the end of the hose, pressure is calculated at 160 psig. At the end of the conical section preceding the orifice, calculated pressure is 45 psig. Only 0.014" upstream the pressure is 87 psig. This rapid pressure change could be brought into agreement with measurements by reducing the fluid viscosity, increasing grid density, or if actual geometry in this section is slightly different from the computational geometry and adjustments were made. Since the thermal aspects of the phase change have not been addressed yet, the calculated temperature in the nozzle remains ambient.

The maximum measured velocity (average for first second) for each tank was compared to the calculated velocity for the location corresponding the tank measurement location. In general, the velocities are reasonably close in the first 25 mm, and after that, the CFD values remain higher than measurements. Measurements indicate that jet velocities should decay more rapidly. The CFD velocities in this region are affected by mixing with the nitrogen free-flow and the resulting jet spreading. For mass continuity, CFD velocities would only decrease to the measured velocities at 75 mm if the density were higher or the jet were wider. Adjustments to viscosity and/or pressure vs. density near atmospheric pressure might achieve the needed reduction. It may also be significant that the measurements are for liquid droplets while the CFD results are for a homogeneous fluid. Droplet acceleration and drag are not considered.

Table 4. Velocity Comparison

Tank	Axial Position (mm)	Radial Position (mm)	Avg Initial Velocity (m/s)	Calculated Velocity (m/s)
6	2.5	12.6	49.1	40.0
1	25	11	50.7	56.2
4	50	0	36.7	44.4
5	50	14	28.2	43.9
3	75	0	21.1	45.0
2	75	15.9	23.1	35.7

CONCLUSIONS

This Phase II project has gotten a good set of benchmark data which quantifies relevant mass flow, pressures, temperatures, and velocities during discharge of a 20 pound halon 1211 fire extinguisher. The Phase I CFD model for the fire extinguisher has been improved to more accurately reflect the pressure-density relationship over the range of pressures encountered. The cavitating liquid approach was replaced with a gas-gas approach using a customized density source code.

Further code and model enhancements would continue to improve the agreement between CFD analysis and benchmark data. The phase change mechanism needs to be refined to account for the measured temperature drop in the nozzle. Incorporating the change in specific heat from liquid to gas state would result in a more realistic temperature drop. The effects of varying viscosity and grid density should also be investigated. Since the capability to include dissolved nitrogen was incorporated, the impact of varying amounts of nitrogen in the halon could be calculated. Once a good level of agreement is achieved, other liquids could be analyzed by inputting their properties. An external model could also be developed which calculates the gas and liquid trajectory relative to a fire plume and/or physical surroundings.

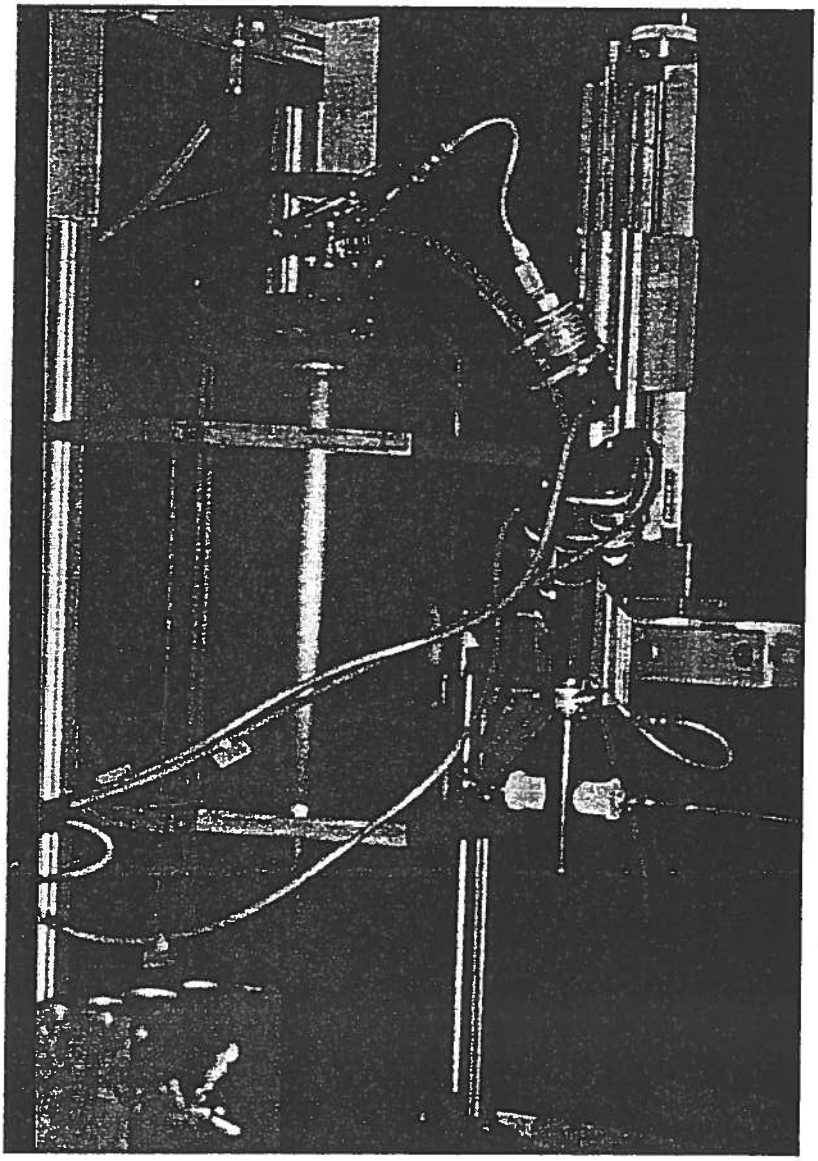

Figure 1. Test Set-up

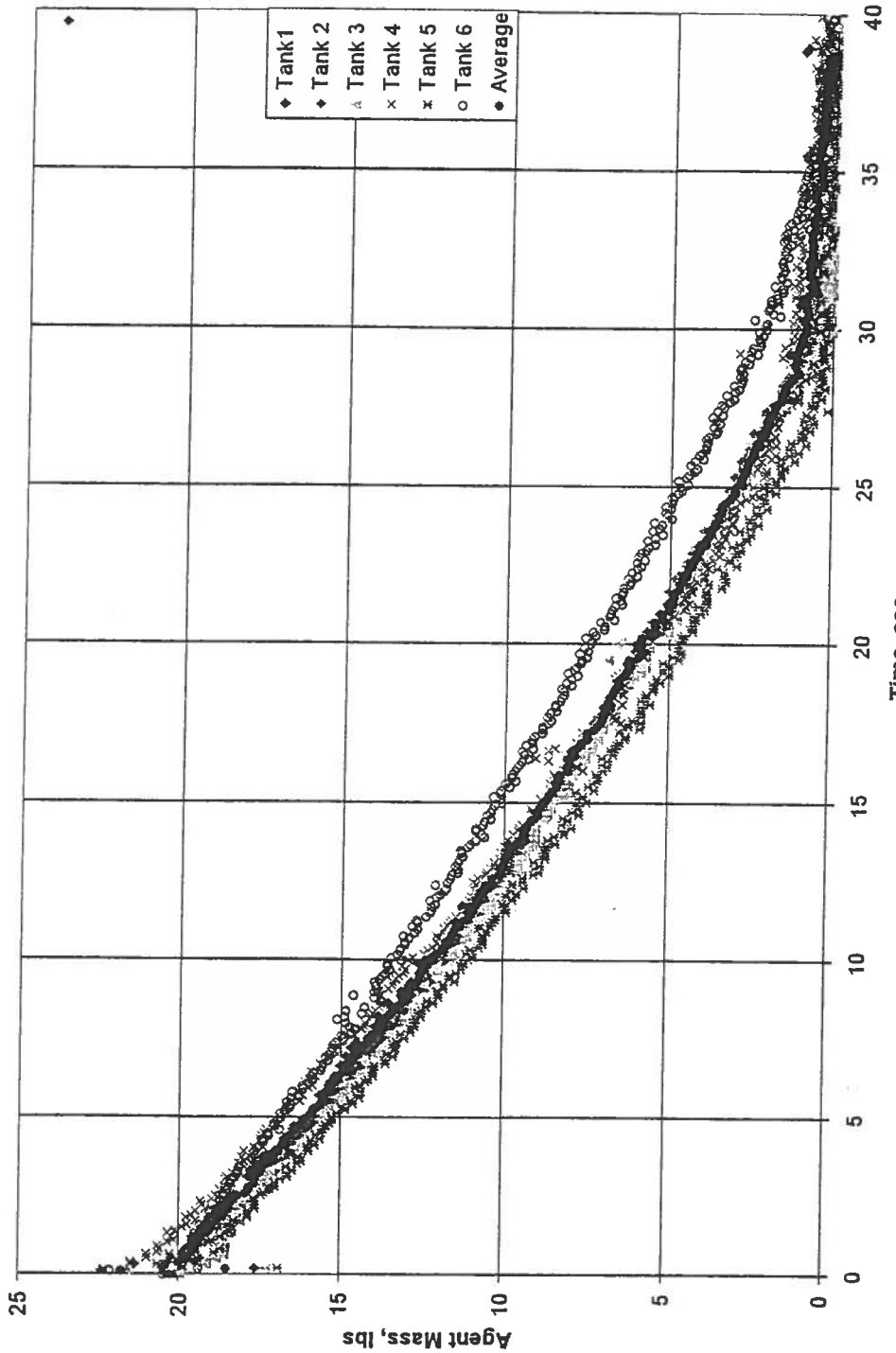

Figure 2. Halon Mass Decay during Discharge

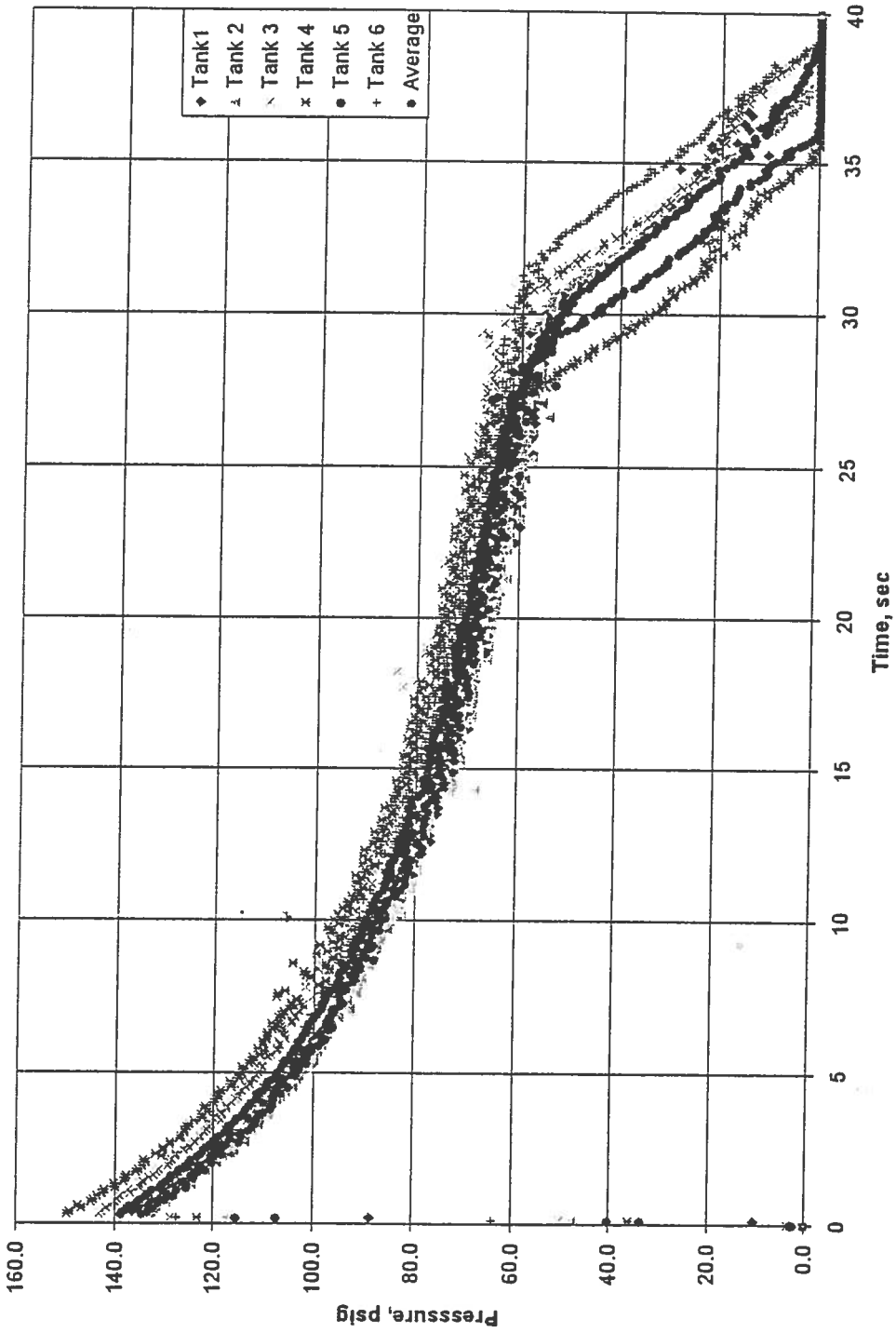

Figure 3. Pressure Downstream of Valve

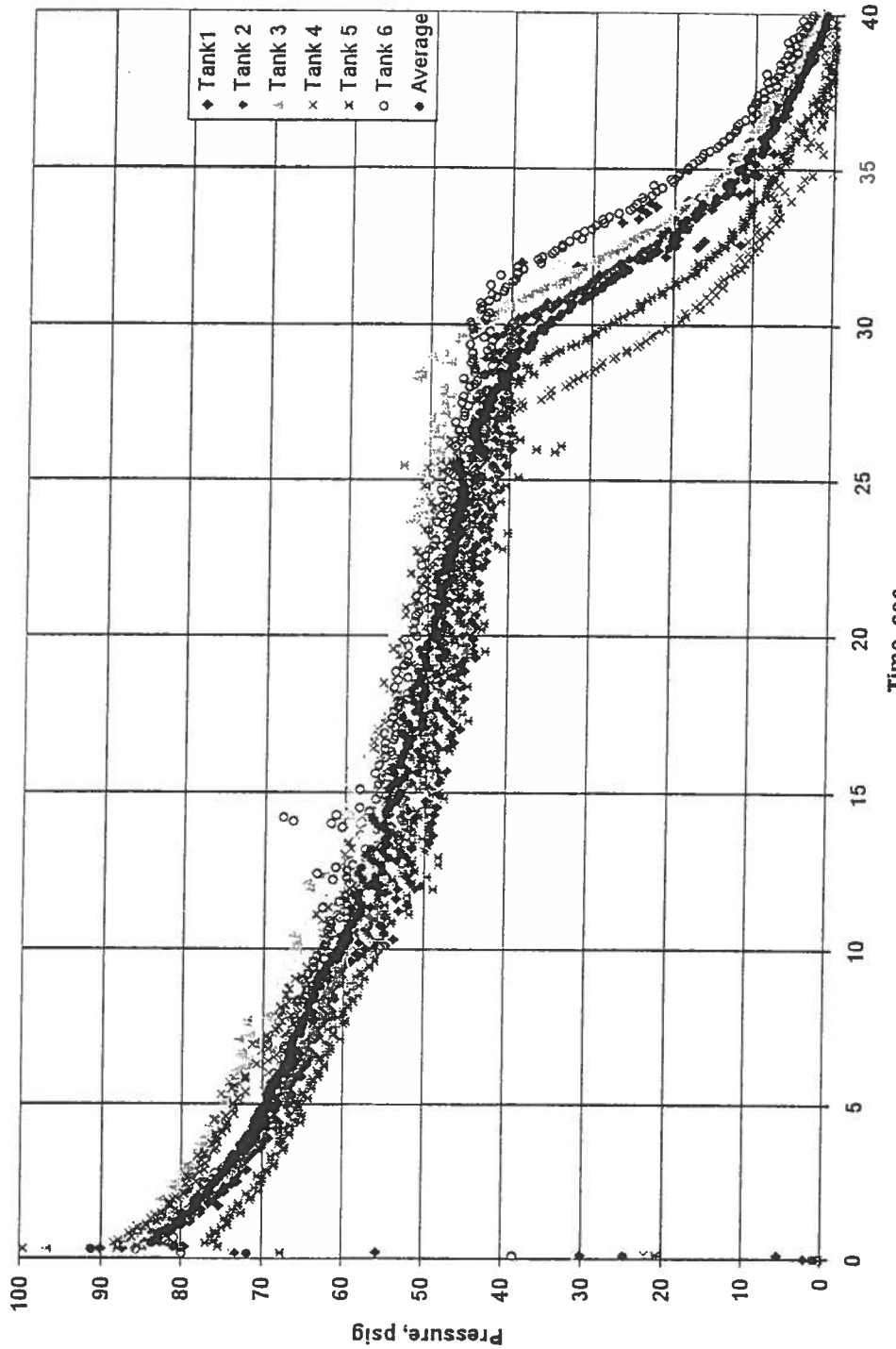

Figure 4. Pressure in Orifice

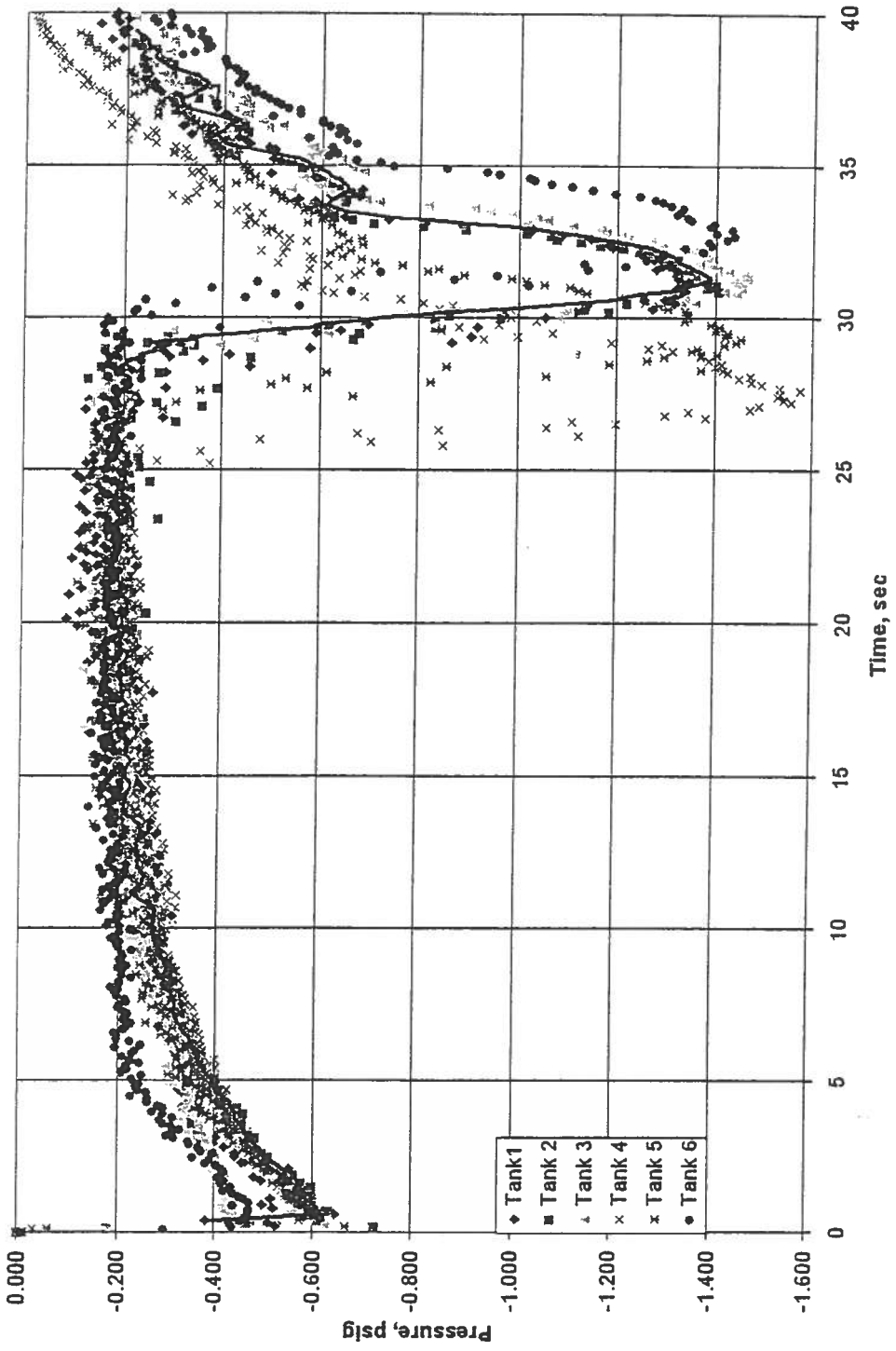

Figure 5. Pressure in Discharge Nozzle

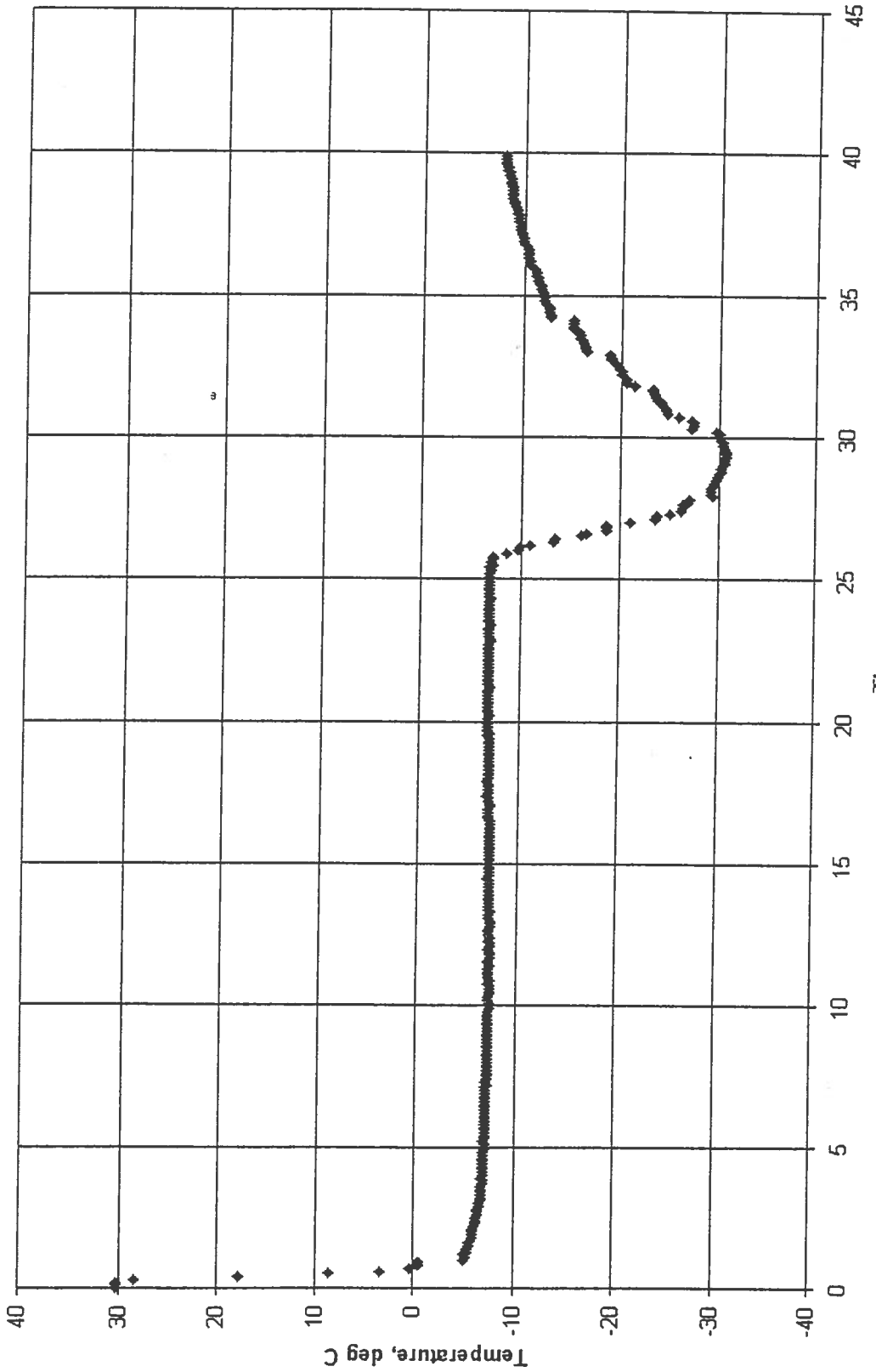

Figure 6. Tank 4 Nozzle Temperature

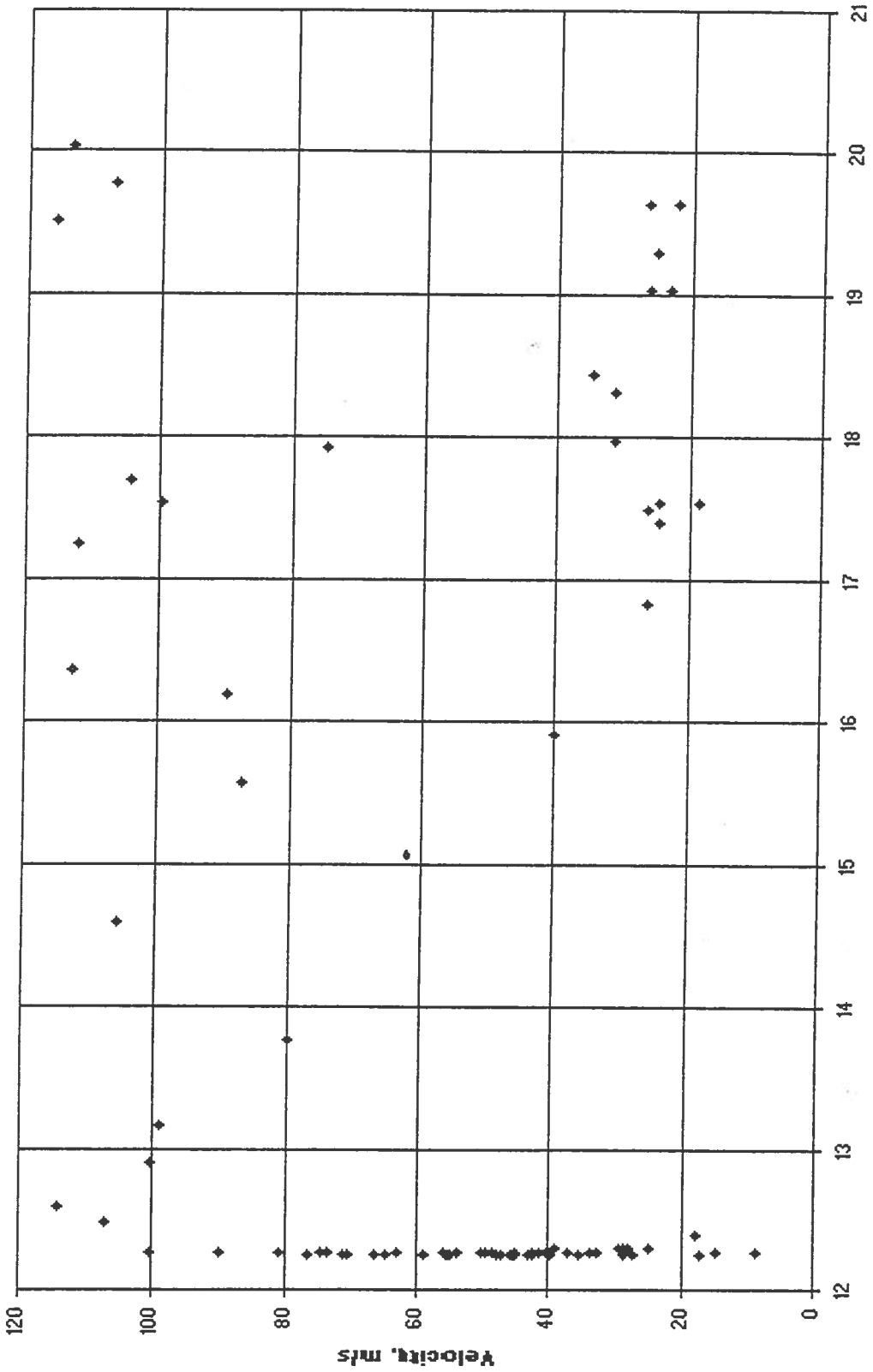

Figure 7. Velocity Measurements for Tank 1; See Table 1 for measurement location

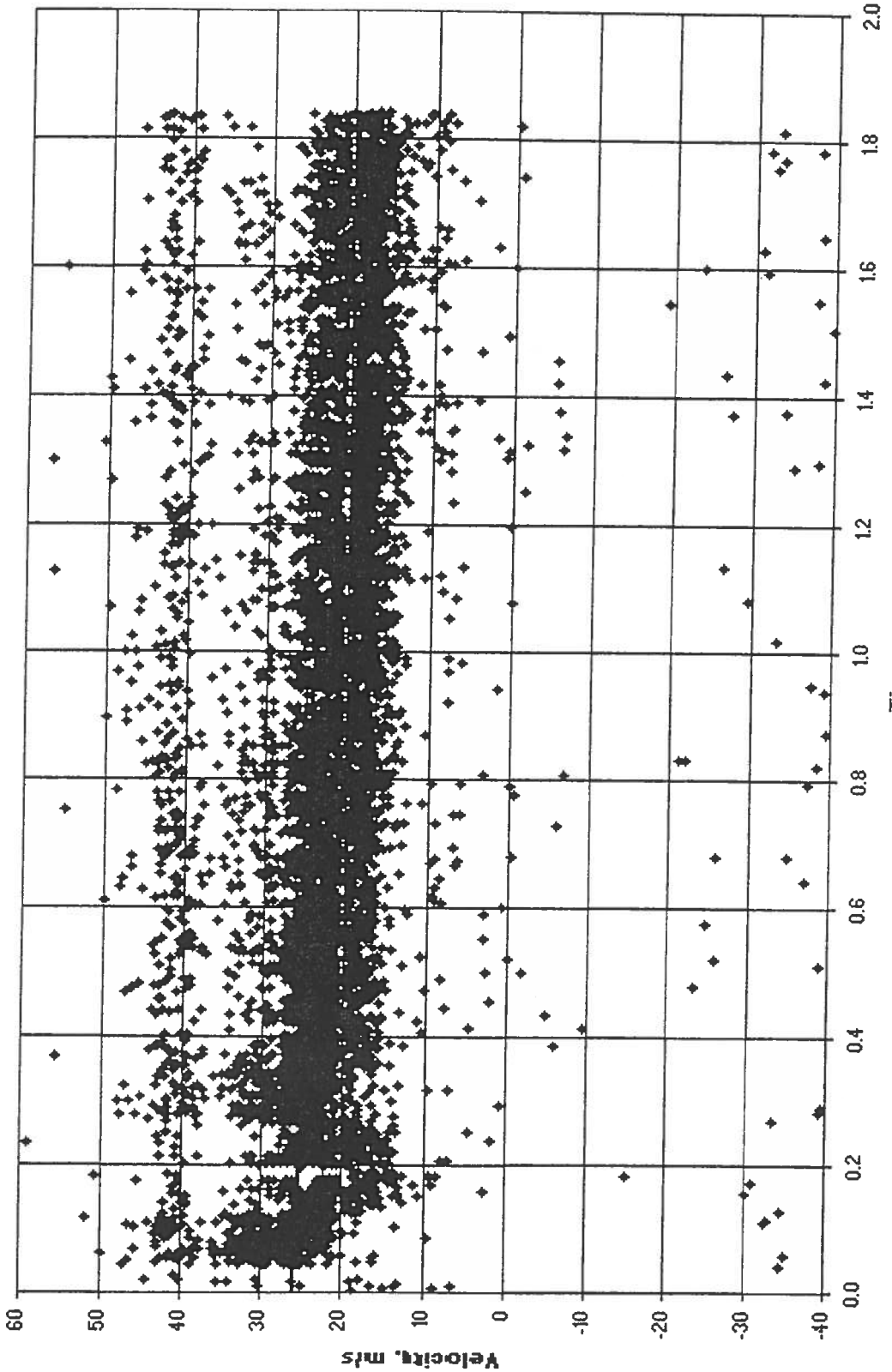

Figure 8. Velocity Measurements for Tank 2; See Table 1 for measurement location

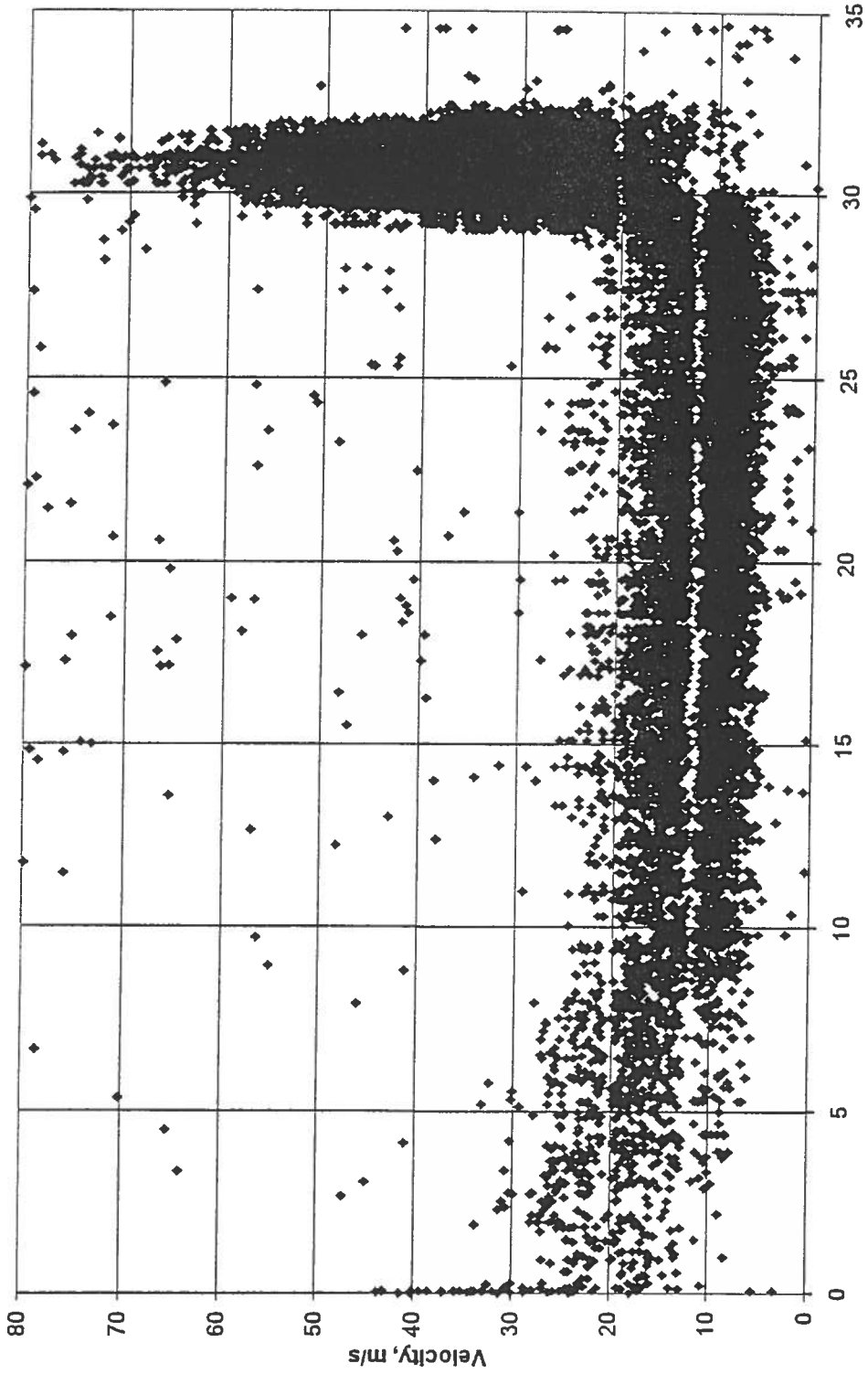

Figure 9. Velocity Measurements for Tank 3; See Table 1 for measurement location

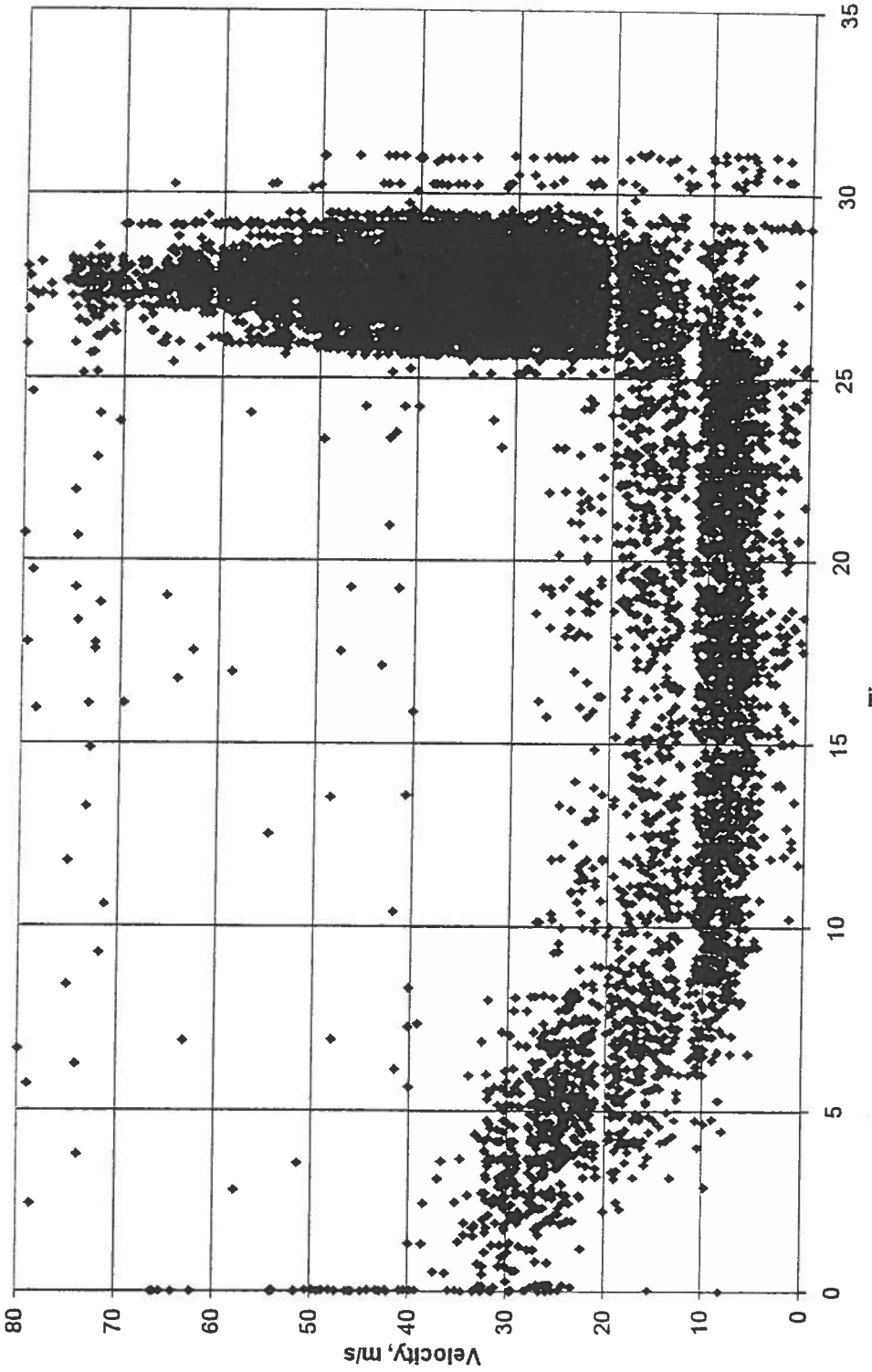

Figure 10. Velocity Measurements for Tank 4; See Table 1 for measurement location

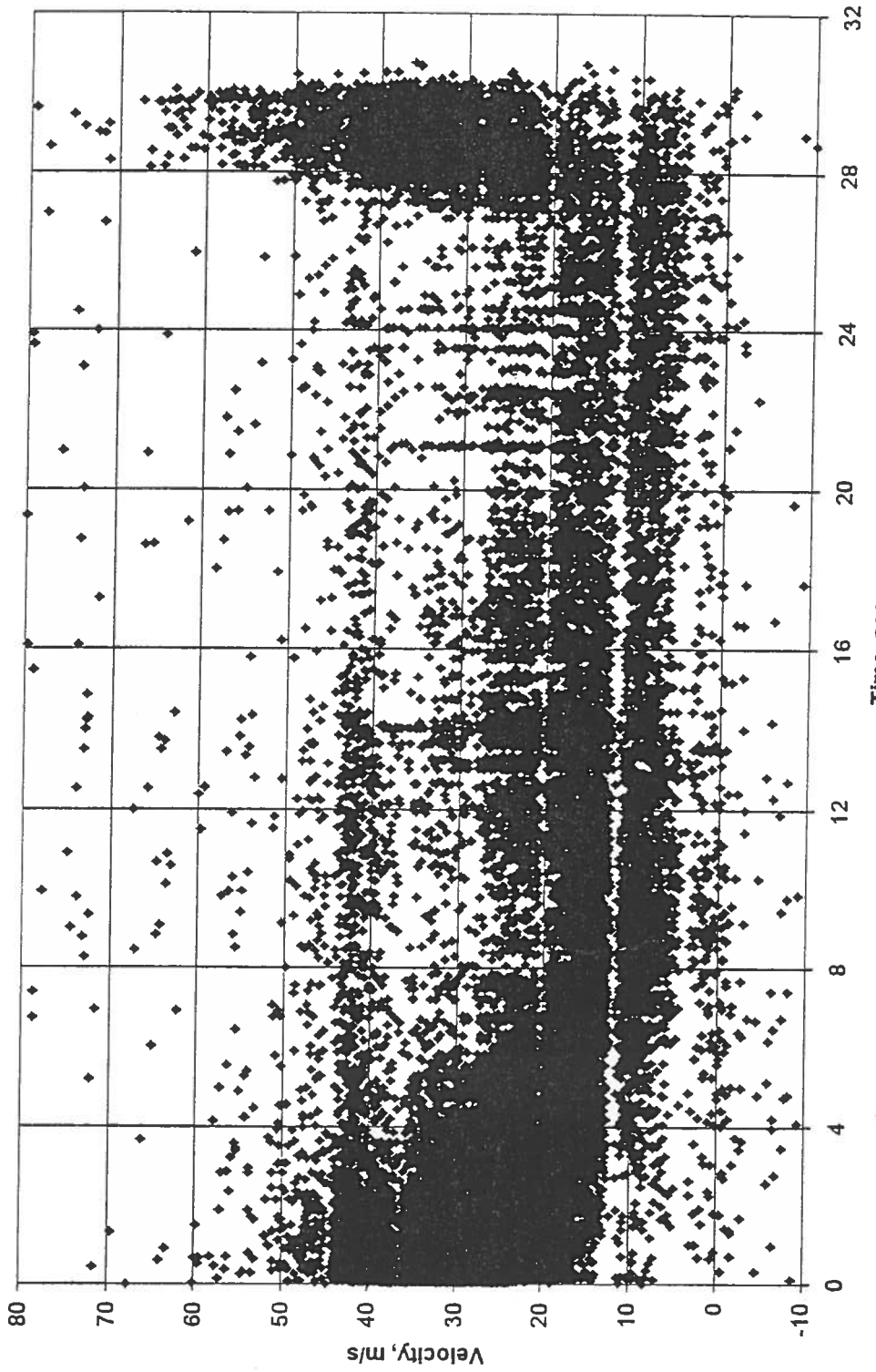

Figure 11. Velocity Measurements for Tank 5; See Table 1 for measurement location

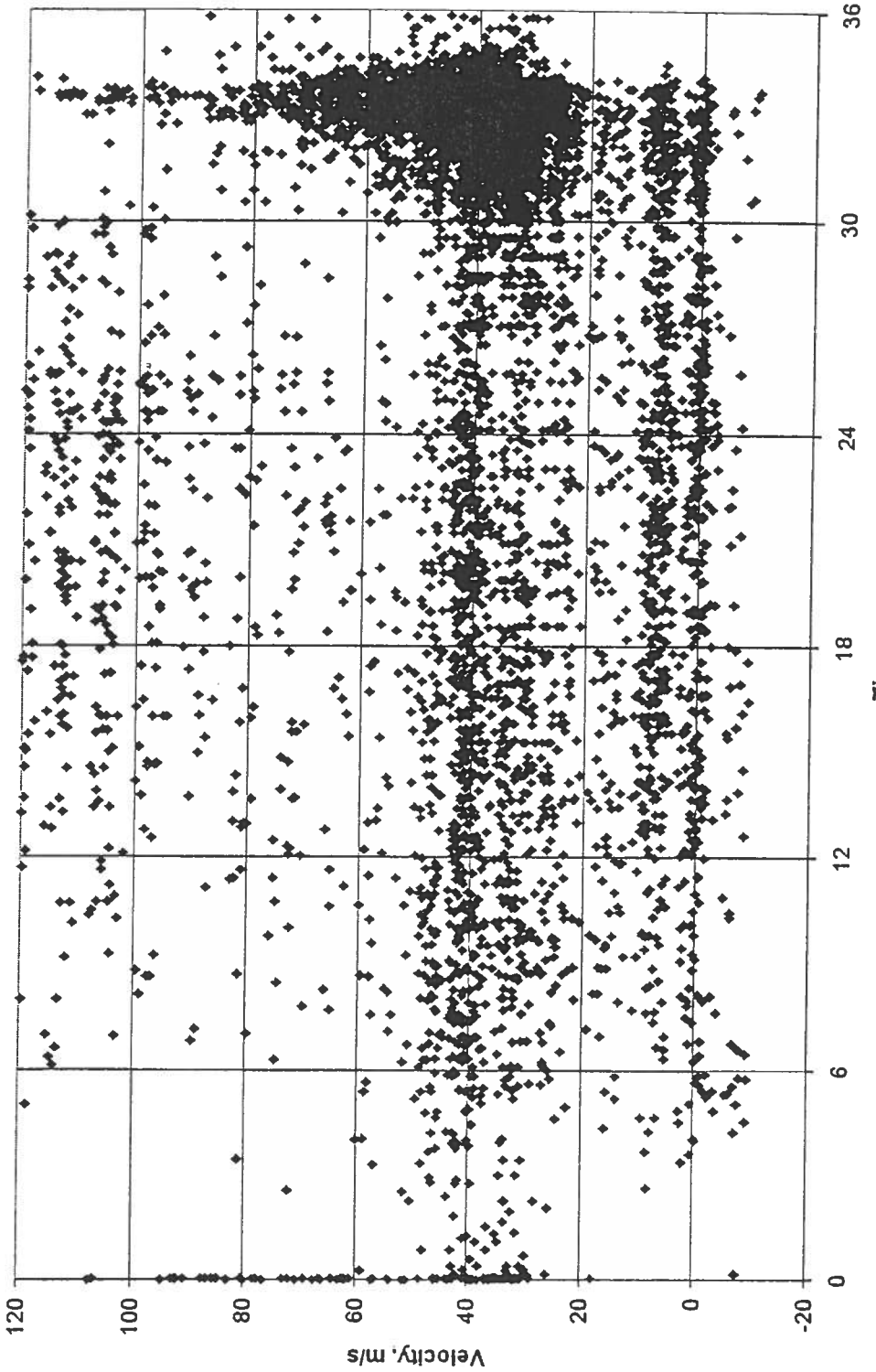

Figure 12. Velocity Measurements for Tank 6; See Table 1 for measurement location

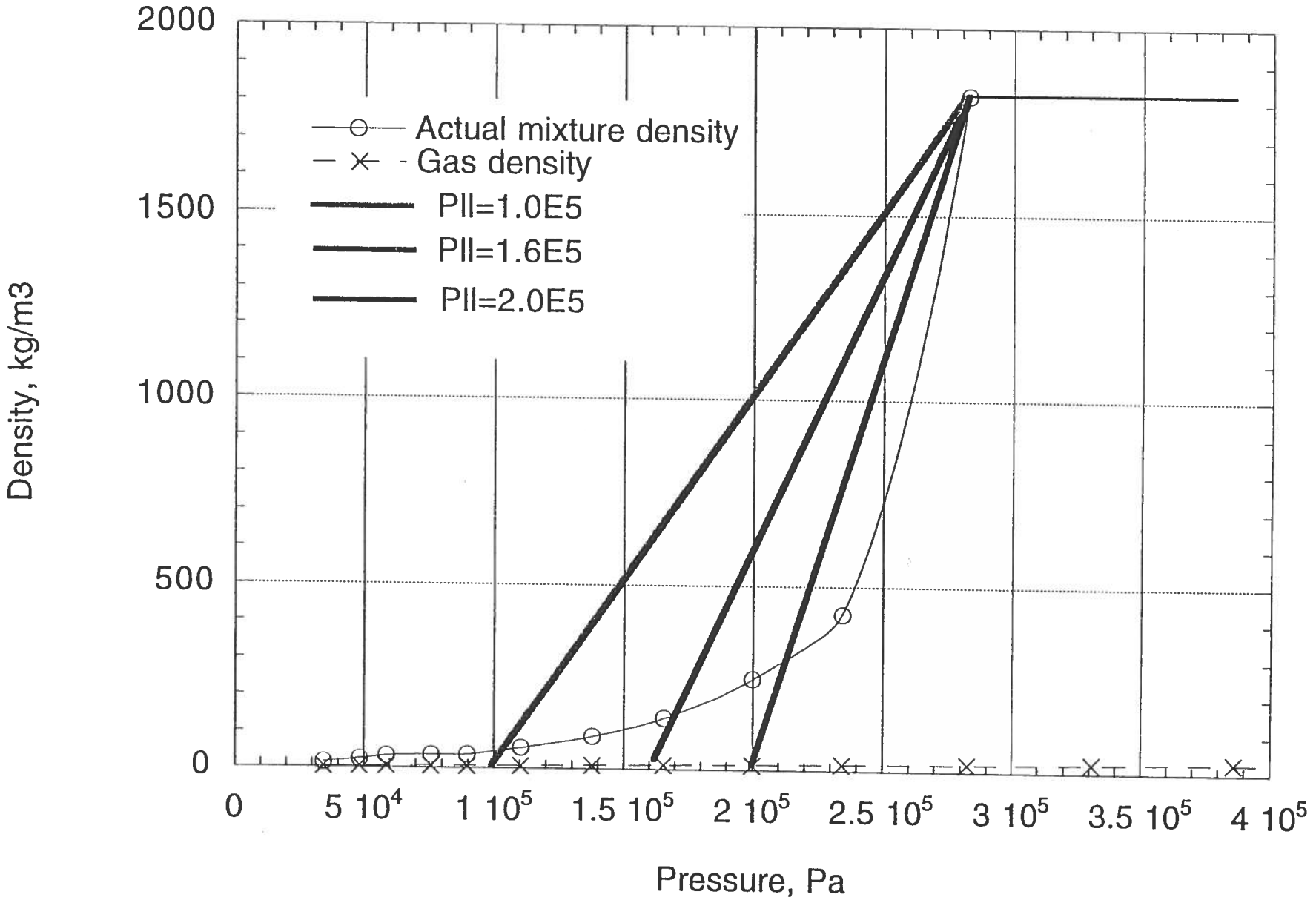

Figure 13. Halon 1211 Density vs. Pressure during Phase Change is Approximated Linearly

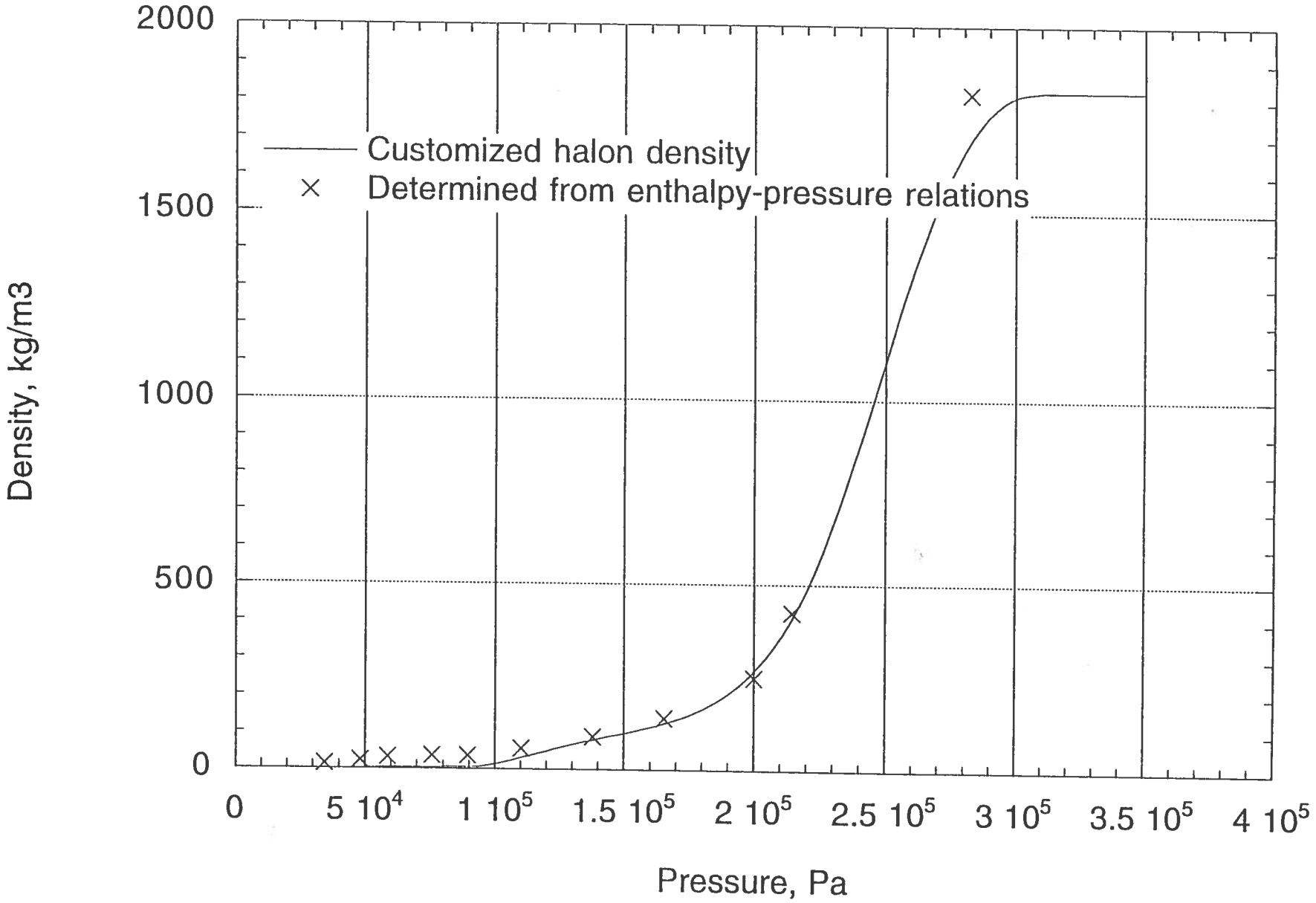

Figure 14. Customized Density Coding Accurately Reflects Values Calculated from Enthalpy

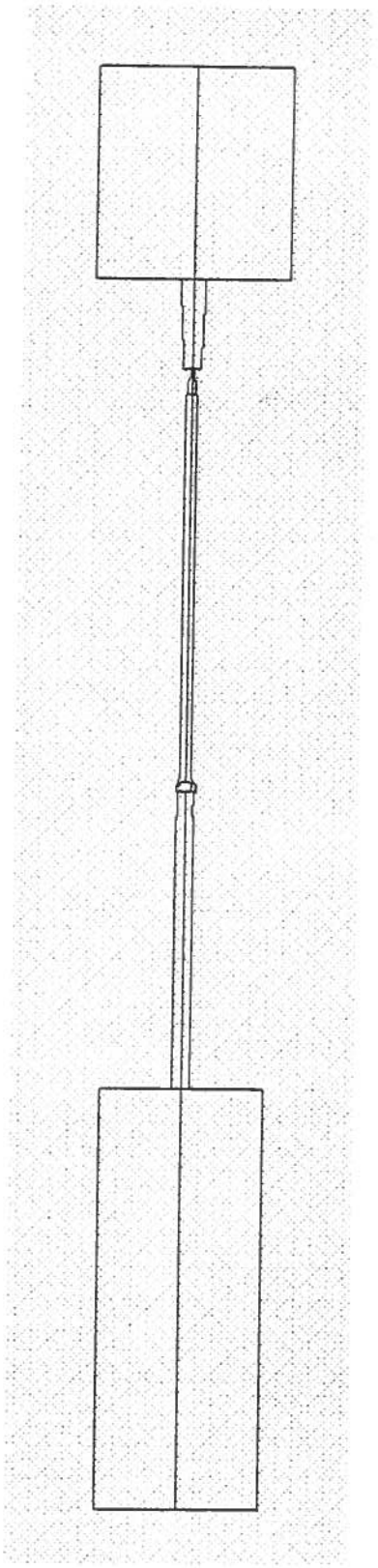

Figure 15. Fire Extinguisher Geometry

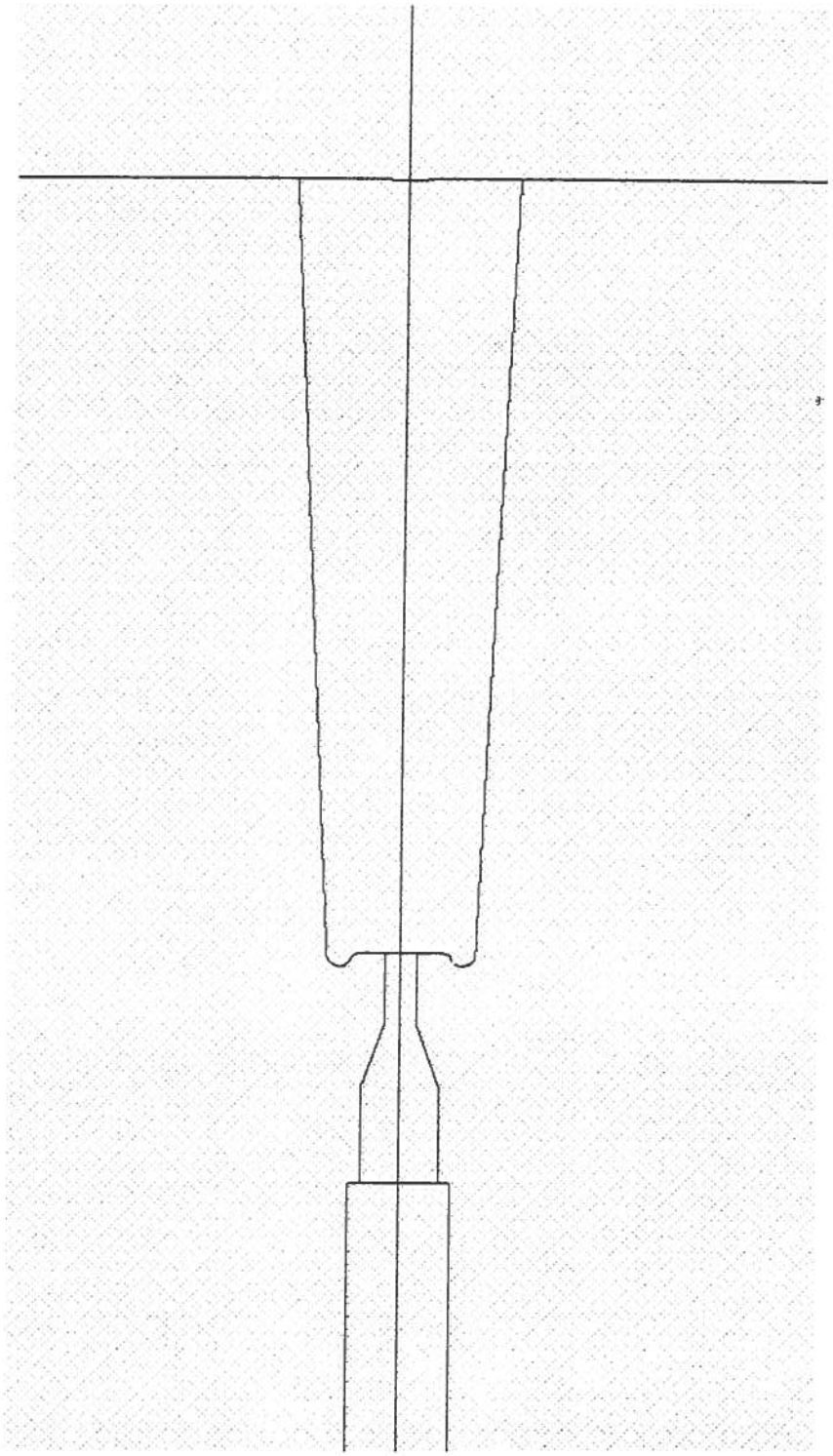

Figure 16. Fire Extinguisher Nozzle Geometry

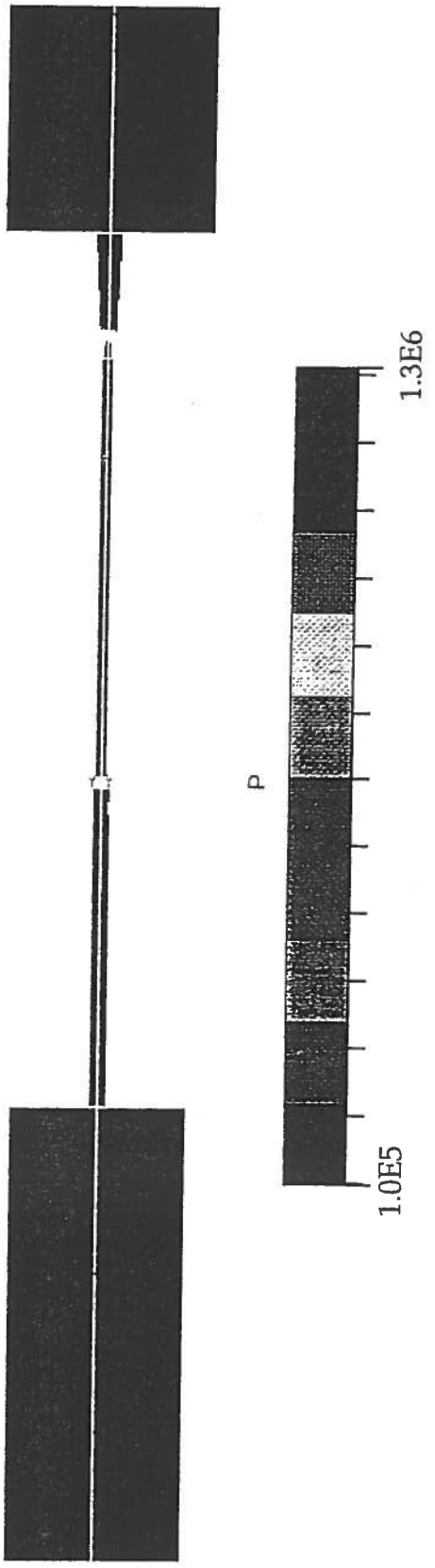

Figure 17. System Pressure Field

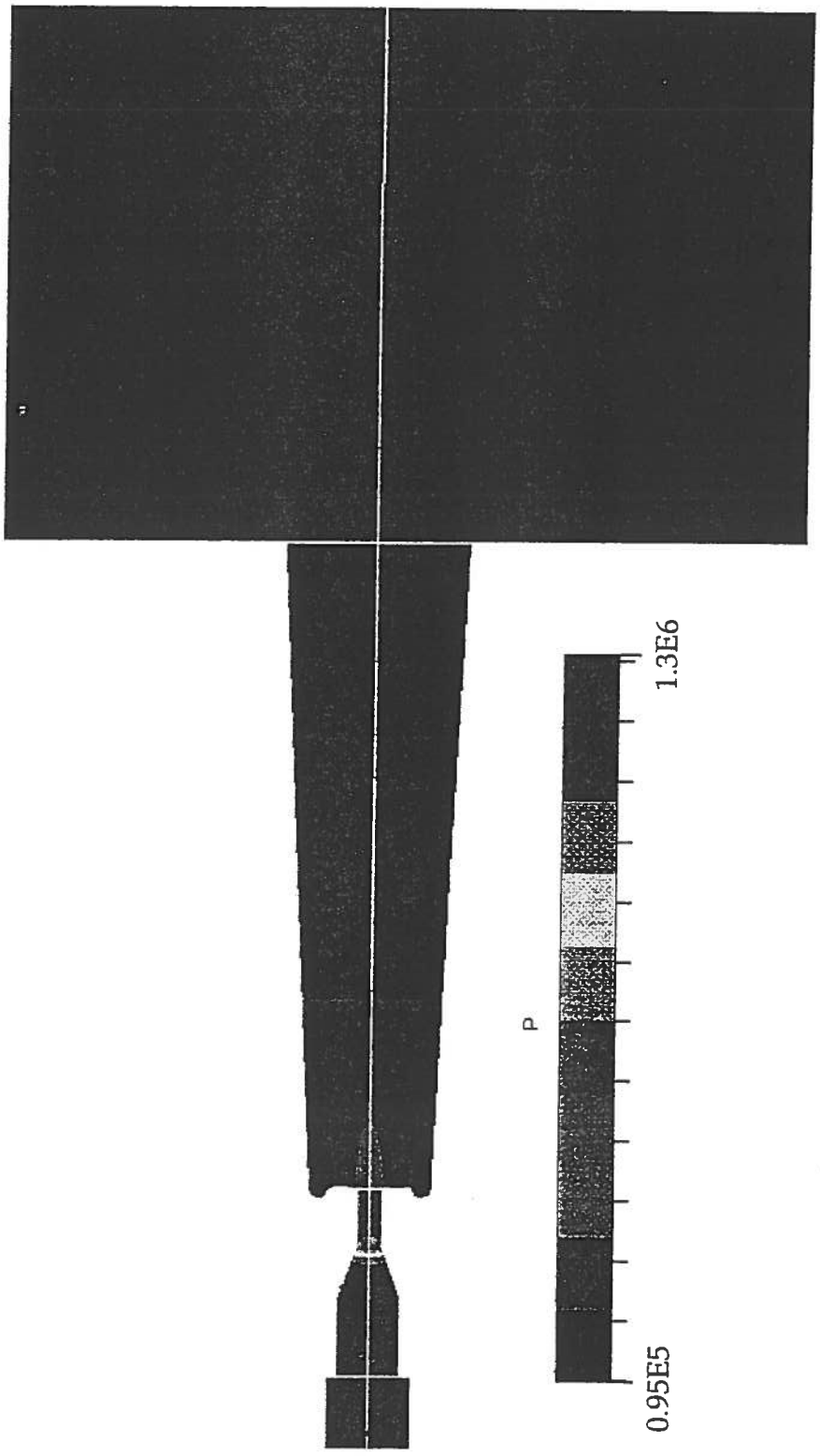

Figure 18. Most Pressure Drop Occurs in Orifice

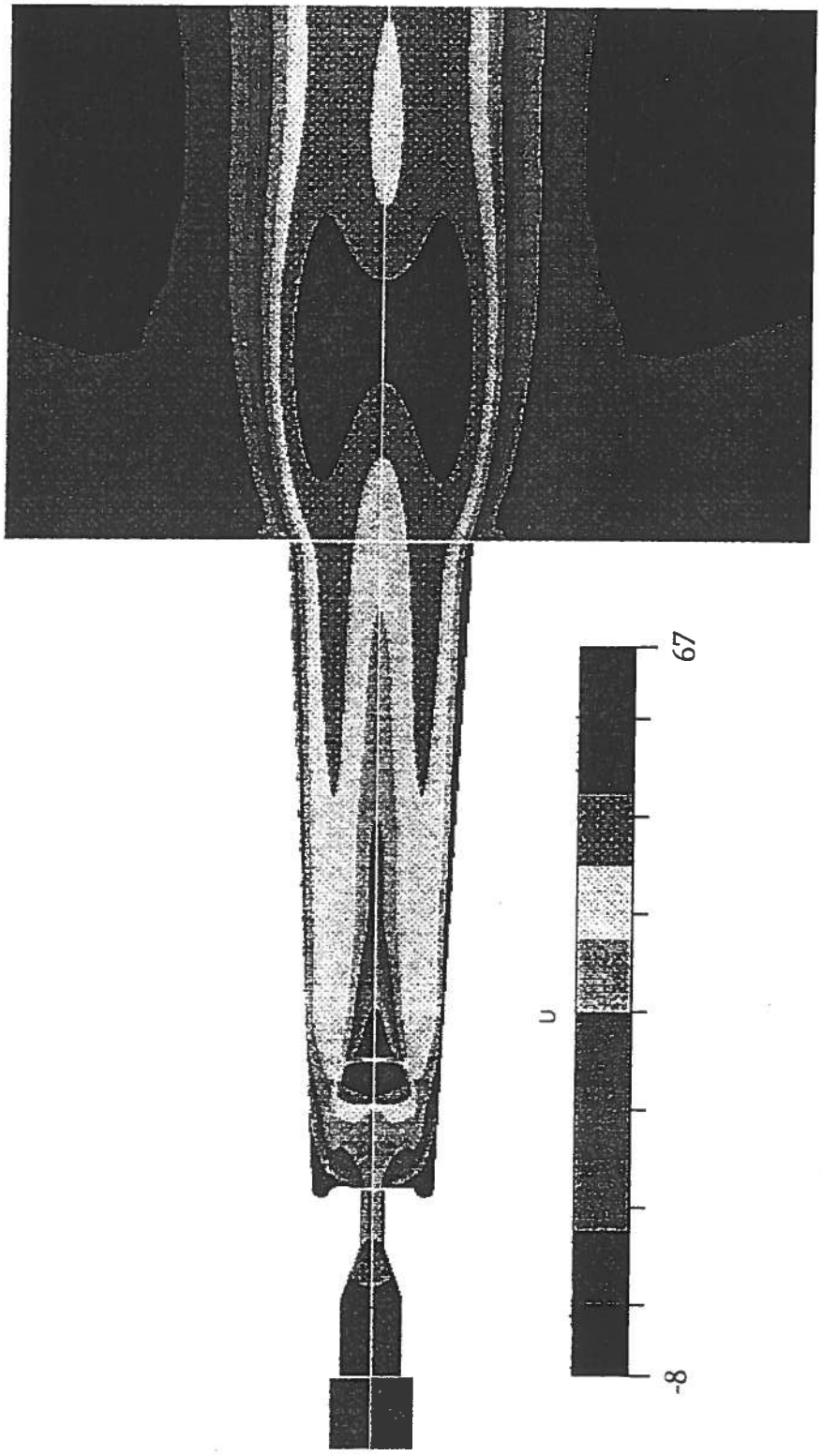

Figure 19. Velocity Increases in Orifice and Nozzle

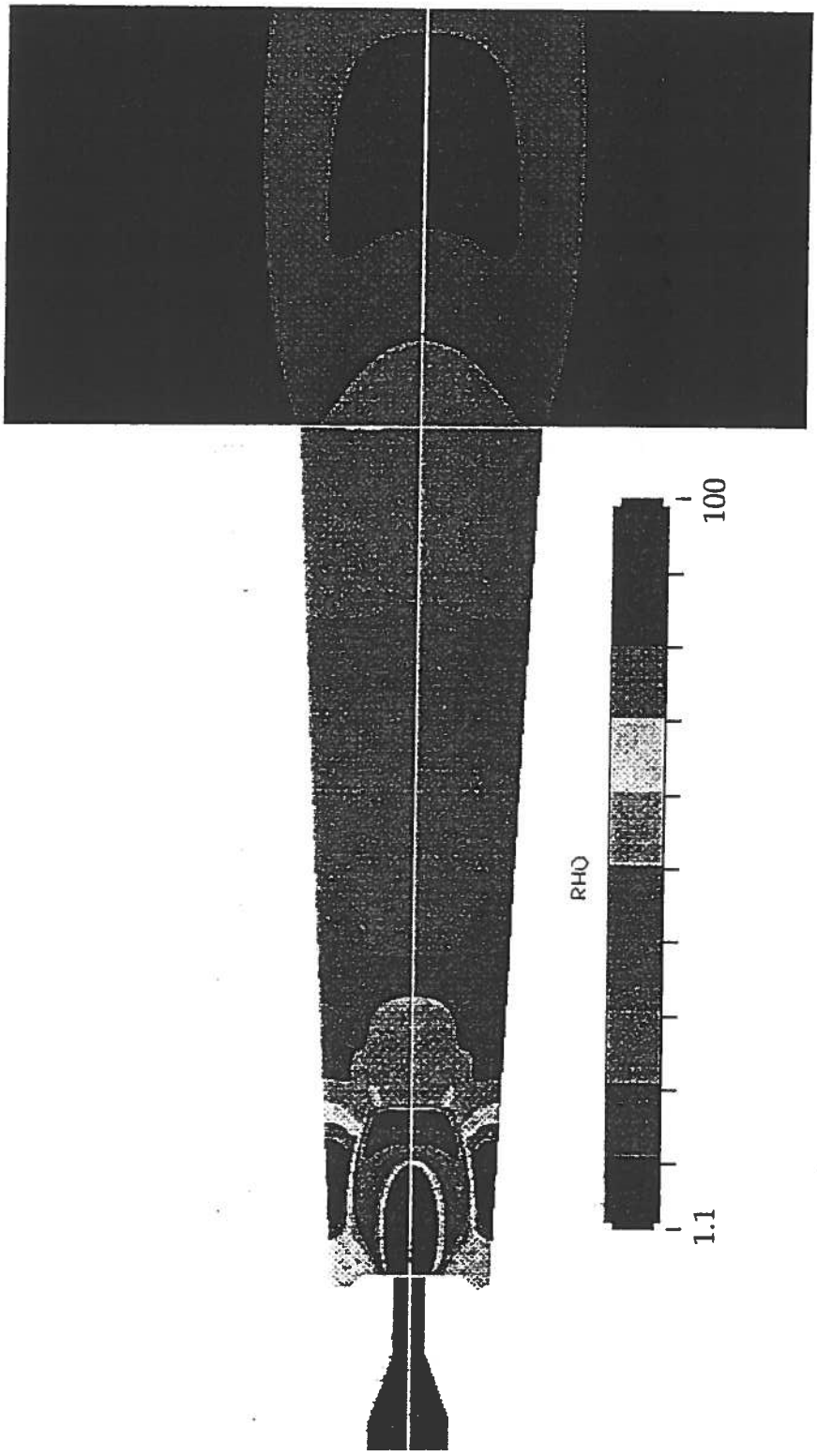

Figure 20. Density Variation Reflects Shock-like Structure